이학석사 학위논문

심장 동종이식혈관병증에서 miRNA-34c-5p 와 miRNA-142-5p 의 역할

The Differential Roles of miRNA-34c-5p and miRNA-142-5p in Cardiac Allograft Vasculopathy

울 산 대 학 교 대 학 원

의 학 과

한 재 석

심장 동종이식혈관병증에서

miRNA-34c-5p 와 miRNA-142-5p 의 역할

지 도 교 수 김 재 중

지 도 교 수 김 나 영

이 논문을 이학석사학위 논문으로 제출함

2019 년 08 월

울 산 대 학 교 대 학 원

의 학 과

한 재 석

한 재 석의 이학석사학위 논문을 인준함

심사위원 정 동 환 (인)

심사위원 김 재 중 (인)

심사위원 김 나 영 (인)

울 산 대 학 교 대 학 원

2019년 08월

Contents

그림목차

Abstract

Background: Cardiac allograft vasculopathy (CAV) restricts long-term survival after cardiac transplantation. Microarray analysis was previously performed to select miRNAs upregulated in the biopsy sample from a heart transplant patient with CAV, compared with that of a healthy heart transplant patient. Among them, miR-142-5p was upregulated in primary human umbilical vein endothelial cells (HUVEC) and an established HUVEC line, when allogeneic immune responses were elicited by co-culture with unrelated blood mononuclear cells, while miR-34c-5p was upregulated in response to hypoxia. Therefore, the aim of this study was to investigate the roles of the miRNAs involved in allogeneic immune responses and hypoxia *in vitro* and *in vivo*.

Methods: HUVEC and blood cells were co-cultured to induce allogeneic immune response. Lentiviral infection and miRNA inhibitor transfection to HUVEC were performed to investigate the effect of overexpression and knock-down. Mice were sacrificed 7 days after skin graft and 1 or 3 days after hind limb ischemia. Real-time qPCR was used to evaluate the expression of miRNA and mRNA. The expression of B7-1 (CD80), B7-2 (CD86), MHC class

I (HLA-ABC), and II (HLA-DR) on the surface of HUVEC and blood cells were assessed by flow cytometry. Protein expression in the skin graft and the hind limb tissue were determined by western blotting.

Results: I found that miR-142-5p was upregulated by allogeneic immune responses using HUVEC coculture with blood cells and a mice skin graft model. The results of flow cytometry show that MHC class I (HLA-ABC) and MHC class II (HLA-DR) positive cell populations and mean fluorescence intensities were increased by allogeneic immune response. In addition, the expression MHC class II gene (H2-Aa) was also upregulated in the allogeneic skin graft. The 3' UTR of *ZEB1* had a 3 binding sites to miR-142-5p and ZEB1 mRNA and protein level were downregulated by allogeneic immune response *in vitro* and *in vivo*. In the miR-142-5p-overexpressed HUVEC, ZEB1 was downregulated, whereas ZEB1 was upregulated in the miR-142-5p-inhibited HUVEC. Furthermore, miR-34c-5p was upregulated in HUVEC by dysoxia and a hind limb ischemia model. The 3' UTR of *c-MYC* had a 3 binding sites to miR-34c-5p and c-MYC protein level was downregulated in miR-34c-5p-overexpressing HUVEC.

Conclusion: I found that miR-142-5p and miR-34c-5p were upregulated by allogeneic

immune responses and by hypoxia respectively, *in vitro* and *in vivo*. ZEB1 was downregulated by miR-142-5p, while c-Myc was downregulated by miR-34c-5p. These results suggest that the cardiac transplant rejection may be exacerbated by miR-142-5p and miR-34c-5p upregulation and ZEB1 and c-Myc downregulation, respectively.

Introduction

Cardiac transplantation is a surgical treatment that removes a dysfunctional heart in a patient to replace with a healthy one. According to the Korea Centers for Disease Control and Prevention, the number of waiting patients for cardiac transplantation has increased from 70 in 2000 to 577 in 2017 in Korea. The survival rate after cardiac transplantation decrease over the years gradually from 90.44% at 3 months, 85.95% at 1 year to 75.96% at 5 years and 66.03% at 11 years post operation [Annual Report of Korean Network for Organ Sharing in 2017, Korea Centers for Disease Control and Prevention].

Cardiac allograft vasculopathy (CAV), a vascular disease unique to cardiac transplant patients, starts to occur approximately 1 year after surgery and affects the long-term survival [1]. The frequency of CAV, which is a major cause of death in heart transplant patients, is as high as 8% after 1 year, 30% after 5 years, and 50% within 10 years after transplantation [2]. CAV manifests as a fibroelastic proliferation of intima and luminal stenosis [3]. Vascular fibroproliferation of the coronary vasculature and allograft dysfunction were generated by endothelial inflammation and injury which were induced by an immune and nonimmune risk

factors [4]. Nonimmune risk factors, include organ preservation injury, ischemic reperfusion injury, metabolic disorders, cytomegalovirus infection, and immune risk factors are rejection and HLA mismatch [4]. Allograft vasculopathy is a form of Th1-mediated delayed-type hypersensitivity driven by recognition of alloantigens, especially nonself polymorphic forms of class I and II MHC molecules expressed on the surface of the graft-derived luminal endothelial cells [5]. Development of CAV appears to be affected by donor and recipient age, ischemic time, postoperative renal replacement therapy, and high triglyceride levels [6]. From the perspective nonimmunologic risk factors, allograft vasculopathy was influenced by several factors such as cyclosporine A (CsA), the renin-angiotensin and transforming growth factor-beta (TGF-β) system [7]. Other factor in allograft vasculopathy is ischemic time. Endothelial cell injury, cellular and vascular rejection over the release of donor antigens might be influenced by ischemic injury at the time of heart transplantation [8]. Yamani, et al. indicate that increased prevalence of development of coronary vasculopathy is presented in patients with peri-transplant myocardial ischemia followed by fibrosis [8]. Myocardial hypoxia is the outcome of unbalance between oxygen demand and supply. Mitochondrial oxidative

phosphorylation is rapidly stopped when the deprivation of oxygen, with a consequent loss of ATP creation which is an important source for energy metabolism [9]. Hydrogen ions and lactate are accumulated by increase in anaerobic glycolysis for ATP production and that accumulation gives rise to interdiction of glycolysis and intracellular acidosis [9]. Oxidative injury from the production of reactive oxygen species (ROS) is launched by myocardial reperfusion [10]. Oxygen homeostasis is regulated by hypoxia-inducible factor 1 (HIF-1) which supervises both the transport and use of O_2. Some of the target genes of HIF-1 as a transcription factor are secreted factors and cell surface receptors controlled O_2 delivery by adjusting angiogenesis and vascular remodeling [11].

MicroRNAs (miRNAs) have been suggested as biomarkers for graft rejection or transplant dysfunctions [12, 13], as they are critical regulators of the mammalian immune system such as inflammation, innate and adaptive immunity, and infection [14]. As 20-24 nucleotides long non-coding RNA molecules, miRNAs inhibit translation and destabilize mRNA molecules, negatively regulating gene expression [15-17]. Many protein coding genes are regulated by miRNAs wherein multiple genes are targeted by individual miRNA and

multiple miRNAs target individual gene. Gene silencing is induced by binding of mature miRNA to the target messenger RNA (mRNA) in the 3′ untranslated region (UTR), thereby reducing translation of the target mRNA [18].

Sui, et al. analyzed miRNA profiles of the biopsy samples from renal transplant patients with acute rejection for the first time [19], where miR-320 is upregulated and miR-324-3p is downregulated in patients with acute rejection. In a murine cardiac transplant model, miR-182 present in the graft, blood cells, and plasma is suggested as a biomarker for graft rejection [20]. More recently; miR-21, miR-142-3p, miR-142-5p, miR-1461, miR-146b, miR-155, miR-222, miR-223, and miR-494 are found to be upregulated during acute cellular rejection in human and mouse grafted hearts [21]. miR-21 promotes fibrosis in mice with an acute cardiac rejection [22]. Upregulation of miR-22 contributes to mitochondrial oxidative damage and cell injury induced by ischemia-reperfusion through targeting Sirt1 and PGC1α in cardiomyocytes [10]. The expression of the miR-199a ~ 214 cluster under cardiac stress via the Hif1α/Twist1 pathway targets PPARδ and impairs mitochondrial fatty acid oxidation [23]. The mice deficient of miR-155 resist cardiac rejection, regulating the Th1/Th17 axis [24].

There are limited studies emphasizing the role of miRNAs in CAV patients, which report an increase in the expression of miR-21-5p, miR-92a-3p, miR-92a-1-5p, miR-126-3p, miR-126-5p, and miR-628-5p in the plasma of the CAV patients more than 5 years post operation [25, 26]. Nonetheless, these studies did not fully investigate the role of miRNAs in CAV using *in vivo* and *in vitro* experimental model systems.

Therefore, this study was set up to elucidate the roles of miR-142-5p and miR-34c-5p in CAV pathogenesis using *in vitro* human and *in vivo* mouse models. This study shows that the upregulation of miR-142-5p targeted ZEB1 expression in allogeneic immune responses and miR-34c-5p targeted c-Myc expression in hypoxia.

Materials & Methods

Cell culture

HUVECs were grown in Medium 200 supplemented with 5% fetal bovine serum (FBS) (Sigma-Aldrich, St. Louis, MO, USA) and low serum growth supplement (Thermo Fisher Scientific, Waltham, MA, USA) in culture dishes precoated with 2% gelatin solution [27]. Cells were cultured in 5% CO_2 at 37°C in an incubator and were used between passages 4 and 7 in this study. An immortalized HUVEC line was purchased from Invitrogen (Lonza, Walkersville, MD, USA) and GFP expressing HUVEC (Angio-proteomie, Boston, MA, USA) were grown in endothelial growth medium-2 (EGM-2) supplemented with 2% FBS and an EGM-2 Bullet Kit (Lonza, Walkersville, MD, USA) in culture dishes pre-coated with 2% gelatin solution. HEK293T cells, a human embryonic kidney cell line (ATCC, Manassas, VA, USA), were maintained in Dulbeco's modified Eagle's medium (DMEM; Hyclone, Logan, UT, USA) supplemented with 10% FBS, 100 U/mL penicillin and 100 μg/mL streptomycin (Corning, Manassas, VA, USA).

Induction of allogeneic immune response *in vitro*

Blood mononuclear cells from healthy volunteers (IRB Approval No. 2012-006) were isolated by density gradient centrifugation using Ficoll-Hypaque (GE Healthcare Bio-Sciences, Björkgatan, Uppsala, Sweden) and resuspended in RPMI1640 medium (Hyclone, Logan, UT, USA), supplemented with 10% FBS (Sigma-Aldrich), 100 U/mL penicillin, 100 μg/mL streptomycin (Corning, Manassas, VA, USA), 5 mM sodium pyruvate (Sigma-Aldrich, St. Louis, MO, USA) and 0.55 mM 2-mercaptoethanol (Thermo Fisher Scientific, Waltham, MA, USA). Primary HUVECs and a HUVEC line were co-cultured with blood cells at a ratio of 1:1 to induce allogeneic immune responses and harvested on day 1 and 3 for further studies.

Murine skin graft model

Murine skin graft was performed following standard protocols with minor modifications [28]. Sex-and age-matched BALB/C as recipient and C57BL/6 mice as allogeneic donor were used (OrientBio, Gyeonggi-do, Korea). Recipients were given C57BL/6 mice tail skin as the graft tissue. Recipient mice were anesthetized with Zoletil 50 (Virbac,

Seoul, South Korea) and Rompun (Bayer Korea, Seoul, South Korea) and shaved around the flank. A graft bed on the left lateral thorax was prepared with fine scissors by removing an area of the epidermis. Skins for grafts 0.8 – 1 cm^2 in area were fitted to the prepared bed with suturing and then covered with Mepitel One (Mölnlycke Health Care, Belrose, Australia), gauze and surgical tape. Mice were sacrificed after 7 days and the skin graft was immediately frozen in liquid nitrogen. The tissues were stored at -80 ˚C until use. All the procedures were approved by IACUC, AMC (Approval No. 2015-12-144).

Induction of hypoxia *in vitro*

To induce hypoxia, 1 x 10^6 HUVECs were seeded in 100 mm dishes one day prior to induction. HUVECs were incubated in hypoxia (1% O_2, 5% CO_2 and 90% N_2) for 24 hours and 72hours.

Murine hind limb ischemia model

The hypoxic condition was investigated in a murine model of hindlimb ischemia in

8-week-old C57BL/6 mice. Animals were anesthetized by Zoletil 50 and Rompun following standard protocols. The superficial femoral artery was ligated with 5-0 polypropylene silk suture, and the skin was closed. Mice were sacrificed after 1 or 3 days and the vessels were immediately frozen in liquid nitrogen. The tissues were stored at -80 ˚C until use.

RNA isolation and quantitative reverse transcription PCR

The expression of miRNA and mRNA were analyzed by real-time qPCR. For HUVEC, total RNA was isolated using TRI-RNA reagent (FAVOGEN, Kaohsiung, Taiwan). Cells were lysed in 1 ml of TRI-RNA reagent by repetitive pipetting. Grafted skins were added into the gentleMACS™ M tube (Miltenyi Biotec, Bergisch Gladbach, Germany) and homogenized in 1 ml of TRI-RNA reagent by gentleMACS™ Dissociator (Miltenyi Biotec, Bergisch Gladbach, Germany). RNA was precipitated from the aqueous phase by mixing with 0.5 ml of isopropanol, incubated at room temperature for 10 min and centrifuged at 12,000 rpm for 15 min at 4 . The supernatant was removed, and the RNA pellet was washed twice with 75% ethanol. The pellet was air-dried and dissolved in diethyl pyrocarbonate (DEPC)-

treated water. miRNA was reverse transcribed with a TaqMan MicroRNA reverse transcription kit (Applied Biosystems, Foster City, CA, USA) using miRNA sequence-specific primers for miR-142-5p. Briefly, for the reverse transcription reactions, 50-100 ng of total RNA were used in each reaction (15 μL) and was mixed with the reverse transcription primer (3 μL). The reverse transcription reaction was performed at 16°C for 30 min, 42°C for 30 min, and 85°C for 5 min. Including U6 as house-keeping gene, miRNA was quantified by real-time qPCR using TaqMan MicroRNA assays and Messenger RNA (mRNA) expression for ZEB1 was quantified by SYBR Green (Applied Biosystems, Foster City, CA) two-step real-time qPCR, using an ABI 7900 Sequence Detection System (Applied Biosystems, Foster City, CA). Primer sequences for real-time qRT-PCR are as follows: human *ZEB1* forward primer: 5′-GCACCTGAAGAGGACCAGAG-3′, reverse primer: 5′- TGCATCTGGTGTTCCATTTT-3′ [29], human *HPRT* forward primer: 5′- CCTGGC GTCGTGATTAGTG-3′, reverse primer: 5′-CAGAGGGCTACAATGTGATGG-3′ [30], Human *HUPO* forward primer: 5′-CCATTCTATCATCAACGGGTACAA -3′, reverse primer: 5′-AGCAAGTGGGAAGGGTAATCC-3′ [31], mouse *Zeb1* forward primer: 5′-

ACCCCTTCAAGAACCGCTTT-3′, reverse primer: 5′-CAATTGGCCACCACTGCTAA-3′ [32], mouse *H2-Aa* forward primer: 5'-CAACCGTGACTATTCCTTCC-3', reverse primer: 5'-CCACAGTCTCTGTCAGCTC-3' [33], mouse *Hprt* forward primer: 5′-TGCCGAGGATTTGGAAAAAGTG-3′, reverse primer: 5′-CAGAGGGCTACAATGTGATGG-3′ [34], mouse *Gapdh* forward primer: 5′-TTGTCAGCAATGCATCCTGCAC-3′, reverse primer: 5′-ACAGCTTTCCAGAGGGGCCATC-3′ [35]. The amplification steps included denaturation at 95°C, followed by 40 cycles of denaturation at 95°C for 15 sec and then annealing at 60°C for 1 min using Applied Biosystems 7900HT Fast Real-Time PCR machine (Applied Biosystems, Foster City, CA, USA). All reactions were performed in triplicate. The results were analyzed by SDS 2.4 (Applied Biosystems, Foster City, CA, USA); the relative expression of miRNA and mRNA was calculated by the $2^{-\Delta\Delta Ct}$ method and was normalized against house-keeping genes.

Production of miR-142-5p and miR-34c-5p expressing HUVEC

The miR-34c-5p- and miR-142-5p-expressing lentiviral vectors were kind gifts from Prof. Young-Ho Ahn (Department of Molecular Medicine, college of Medicine, Ewha Womans University). The PCR product was then ligated into pLVX-Neo vector (modified from pLVX-Puro; Clontech, Mountain View, CA), which was introduced into the cells by lentiviral infection. All transfections were done on 100 mm dishes where 1×10^6 HEK293T cells were plated with 8 ml of DMEM (Hyclone) supplemented with 10% FBS (Sigma-Aldrich) and 1% penicillin and streptomycin (Corning), the night prior to transfection. 6 μg lentiviral vector, 3 μg psPAX2 (Gag-Pro-Plo), and 1 μg pMD2.G (Env) were mixed in 100 μL Opti-MEM (Thermo Fisher Scientific) [Sol 1]. 10 μL Lipofectamine 2000 (Thermo Fisher Scientific) was diluted in 100 μL Opti-MEM (Thermo Fisher Scientific) [Sol 2]. Solution 1 and 2 were mixed after incubation at RT for 15 min, the mixture was further incubated at RT for 15 min. During the incubation, media was changed carefully with 2 ml serum-free DMEM. Transfection mixture was added dropwise to the cell culture dishes. Next morning, media was changed with 2 ml of growth medium for target cells. After 48 h, virus-containing media was collected and filtered the using 0.45 μm syringe filter (Millipore Millex-HV PVDF). One day

prior to infection, 5 x 10^5 HUVEC were seeded in 100 mm dishes. Polybrene (8 μg/ml) was added to the virus and incubated for 10 min, the cell culture media was replaced with the virus-containing media (1-2 ml). After 24 hr, the second infection was performed. Next morning, the media was changed with 2 ml of growth media.

miRNA inhibitor transfection

To inhibit miR-142-5p, 5 x 10^5 HUVEC were seeded in 100 mm dishes one day prior to transfection. After 24 hr, 10 μL Lipofectamine 2000 (Thermo Fisher Scientific) was diluted in 150 μL Opti-MEM (Thermo Fisher Scientific) [Sol 1]. Three μL of 10 μM miRNA inhibitor or negative control (mirVana™ miRNA Inhibitors, Thermo Fisher Scientific) was diluted in 150 μL Opti-MEM (Thermo Fisher Scientific) [Sol 2]. Solution 1 and 2 were mixed and the mixed solution was incubated for 5 min. Transfection mixture was added dropwise to the cell culture dishes. After 2 days, transfected HUVEC were harvested.

Flow cytometry

HUVEC were washed with 1× PBS 3 days after co-culture with blood cells and detached using StemPro™ Accutase™ Cell Dissociation Reagent (Thermo Fisher Scientific, Waltham, MA, USA). Single cells were used for surface flow cytometry staining. Anti-human CD80 (clone 2D10, Biolegend, San Diego, CA, USA), anti-human CD86 (clone IT2.2, Biolegend), anti-human HLA-ABC (clone G46-2.6, BD), anti-human HLA-DR (clone LN3, eBioscience) were used for cell staining. Adequate isotype controls were used as negative control. The results were acquired by CytoFLEX (Beckman Coulter, Brea, CA, USA) and analyzed in FlowJo software Ver 10 (FlowJo, LLC, Ashland, OR, USA).

Western blotting

Mouse skin graft was harvested and chopped in the 1.5 ml tubes. RIPA buffer (Biosesang, Kyungkido, South Korea), 5x Phosphatase inhibitor cocktail set III (Sigma-Aldrich, St. Louis, MO, USA) and 10x Protease inhibitor cocktail (Sigma-Aldrich, St. Louis, MO, USA) were added to the tubes. Skins were mashed with pestle on ice and then incubated for 10 min on ice. Protein-containing supernatant were collected after centrifugation at 14000

rpm at 4 for 15 min. Protein concentrations were measured using Pierce BCA protein assay kit (Thermo Fisher Scientific, Waltham, MA, USA). Total protein of 30 μg per sample was electrophoresed in 8% SDS-PAGE gels and transferred to 0.45 μm polyvinylidene fluoride (PVDF) membranes (GE Healthcare, Pittsburgh, PA, USA). Then, blots were blocked with 5 % Skim milk (Becton Dickinson, Franklin Lakes, NJ, USA) in 1× TBS containing 0.1% Tween 20 (TBST) for 3 hours and incubated with the following antibodies in a 4 ˚C cold room overnight: anti-Zeb1 (polyclonal; Santa Cruz biotechnology, Dallas, TX, USA), anti-c-Myc (polyclonal; Cell Signaling Technology, Danvers, MA USA) anti-β-actin (polyclonal; Bioss, Woburn, MA, USA). The PVDF membranes were washed five times with TBST and incubated with Goat anti-rabbit secondary antibody (Santa Cruz) for 1 hour at room temperature. Finally, protein bands were detected using PicoEPD™ Western Reagent solutions (Elpis Biotech, Daejeon, South Korea) and Image Quant LAS 4000 (GE Healthcare). The band intensities were analyzed using Image Studio Lite software Ver 5.2 (LI-COR Biosciences, Lincoln, NE, USA).

Statistical analysis

Student t-tests and standard deviations (SD) were calculated in MS EXCEL (Microsoft, Redmond, Washington, USA). For the analysis of flow cytometric results, Friedman test (nonparametric ANOVA), Dunn's Multiple comparisons test, and standard error of means (SEM) were calculated by InSTAT 3 (GraphPad Software Inc. La Jolla, CA, USA). *$P < 0.05$; **$P < 0.01$; ***$P < 0.001$.

Result

Expression of miR-142-5p is upregulated in HUVEC and skin graft upon allogeneic immune response.

miR-142-5p was upregulated 11.7-fold in a biopsy sample collected from a CAV patient 1 month post operation, compared with that of a healthy heart transplant patient (Data not shown). Thus, I set up the experiment to investigate the role of miR-142-5p in allogeneic immune responses using primary HUVEC and a HUVEC line by real-time qPCR. Allogeneic immune responses were elicited by incubating with blood mononuclear cells from unrelated healthy donors. As shown in Fig. 1A and B, the miR-142-5p expression was increased approximately by 75 and 95 folds in primary HUVEC and a HUVEC line, respectively, under allogeneic condition at culture day 1, compared with the negative control. The increase was more significant on culture day 1 than day 3. Next, I confirmed the increase of miR-142-5p in a murine skin graft model (Fig. 1C). Allogeneic skin grafts expressed significantly more miR-142-5p, compared with syngeneic ones. In summary, miR-142-5p was upregulated upon allogeneic immune responses in HUVEC cells and murine skin grafts.

Figure 1.

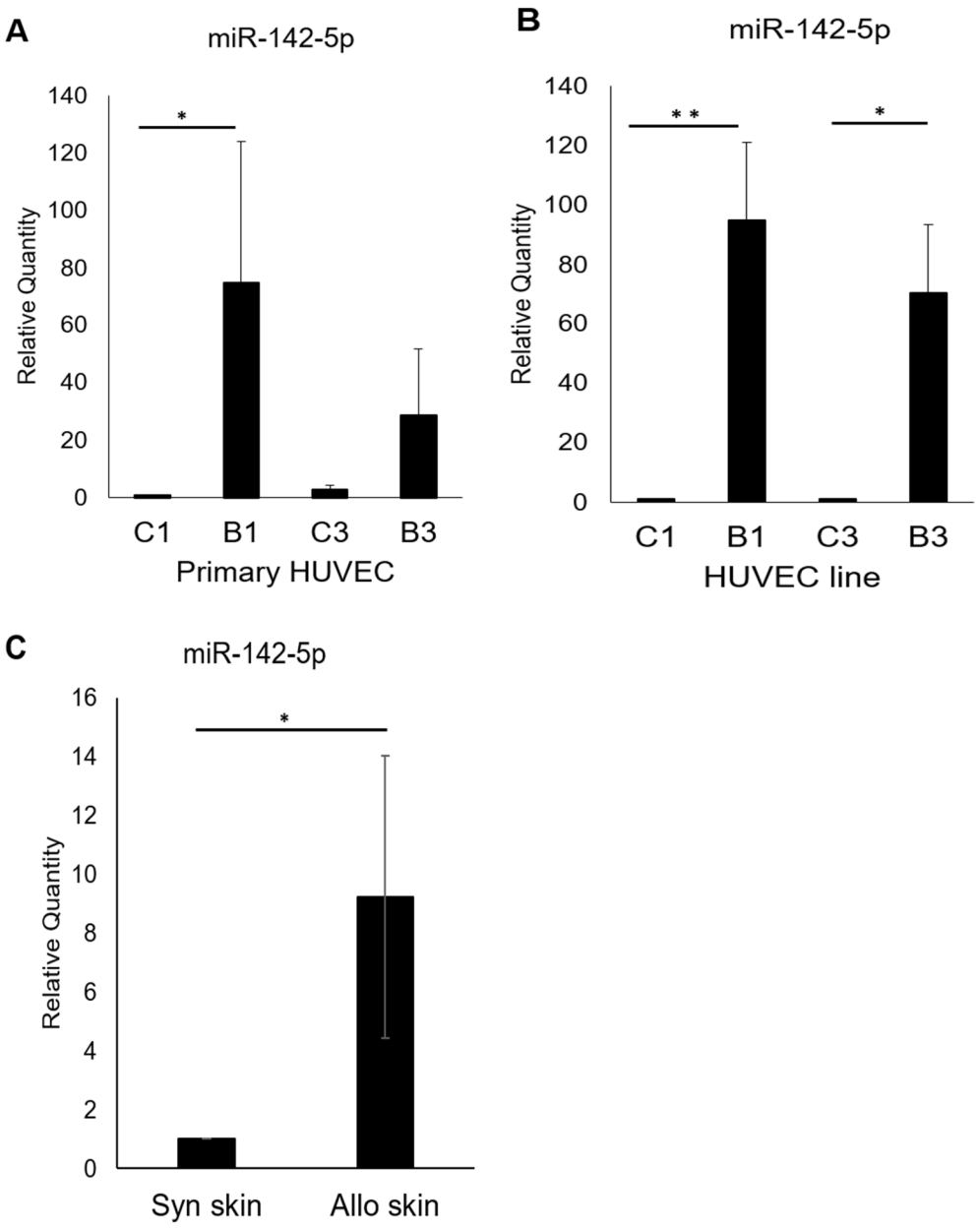
A
miR-142-5p
Relative Quantity
140
120
100
80
60
40
20
0
*
C1
B1
C3
B3
Primary HUVEC
B
miR-142-5p
Relative Quantity
140
120
100
80
60
40
20
0
* *
*
C1
B1
C3
B3
HUVEC line
C
miR-142-5p
Relative Quantity
16
14
12
10
8
6
4
2
0
*
Syn skin
Allo skin

Figure 1. miR-142-5p is upregulated *in vitro* and *in vivo* upon allogeneic immune responses. (A) TaqMan assay was performed to quantify miR-142-5p in primary HUVEC in the presence of allogeneic blood mononuclear cells. The cells were co-incubated for 1 and 3 days. The relative quantities of each miRNA are calculated as the ratios to the endogenous control (mean ± SD). C, the negative control; B, allogeneic blood mononuclear cells. The numeric values represent days in culture. N = 3 for C1 and B1; 4 for C3 and B3. (B) miR-142-5p expression was assessed in immortalized HUVEC as above. N=3. (C) miR-142-5p expression was assessed in the grafted skin in mice as above. Syn, syngeneic; Allo, allogeneic. N = 4. *P < 0.05; **P < 0.01.

Overexpression of miR-142-5p upregulates MHC expression upon allogeneic immune responses

The miR-142-5p-overexpressing HUVEC cells were produced using a lentiviral vector to understand the mechanisms underlying allogeneic immune responses against miR-142-5p. These cells were co-incubated with unrelated blood mononuclear cells for 3 days and the expression of co-stimulatory molecules; B7-1 (CD80) and B7-2 (CD86), and antigen presenting molecules, MHC class I (HLA-ABC) and II (HLA-DR), on the surface of HUVEC was assessed by flow cytometry. As seen in Fig. 2A and B, the percentages of HLA-DR-expressing HUVEC only increased marginally, whereas, There was a further increase of 2.1 folds in miR-142-5p-overexpressing HUVEC co-incubated with unrelated blood cells. This increase was statistically significant. The mean fluorescence indices (MFI) showed more interesting results (Fig. 2A and C); the expression of CD80, CD86, HLA-ABC, and HLA-DR increased in miR-142-5p-overexpressing HUVEC that were co-incubated with allogeneic blood cells. In particular, the expression levels of HLA-ABC and HLA-DR increased significantly by 2.7- and 21-fold, respectively, compared with those in the negative control.

The increase was additive or synergistic when compared with those of miR-142-5p overexpression alone or with addition of allogeneic cells alone. For CD86, the variation among column medians is significantly greater than expected by chance, although the differences between the two specific groups were not significant. The expression of MHC class II was reduced in murine skin graft as well (Fig. 2E). In addition, HUVEC were incubated with blood cells two days after treatment with the miR-142-5p inhibitor. The MFI of HLA-DR$^+$ HUVEC was increased by co-incubated with unrelated blood cells as above, but decreased significantly in miR-142-5p inhibitor-treated HUVEC (Fig. 2D). Furthermore, in order to exclude the possibility that the contaminated blood cells might affect the results, blood cells were collected from the co-incubation and analyzed by flow cytometry. The expression of cell surface markers on the blood cells incubated with non-related HUVEC was compared with those of the blood cells without co-incubation. There were no significant differences in both groups (Fig. 3). In summary, the results suggest that miR-142-5p plays an important role in upregulation of MHC class I and II expression additively to graft rejection.

Figure 2.

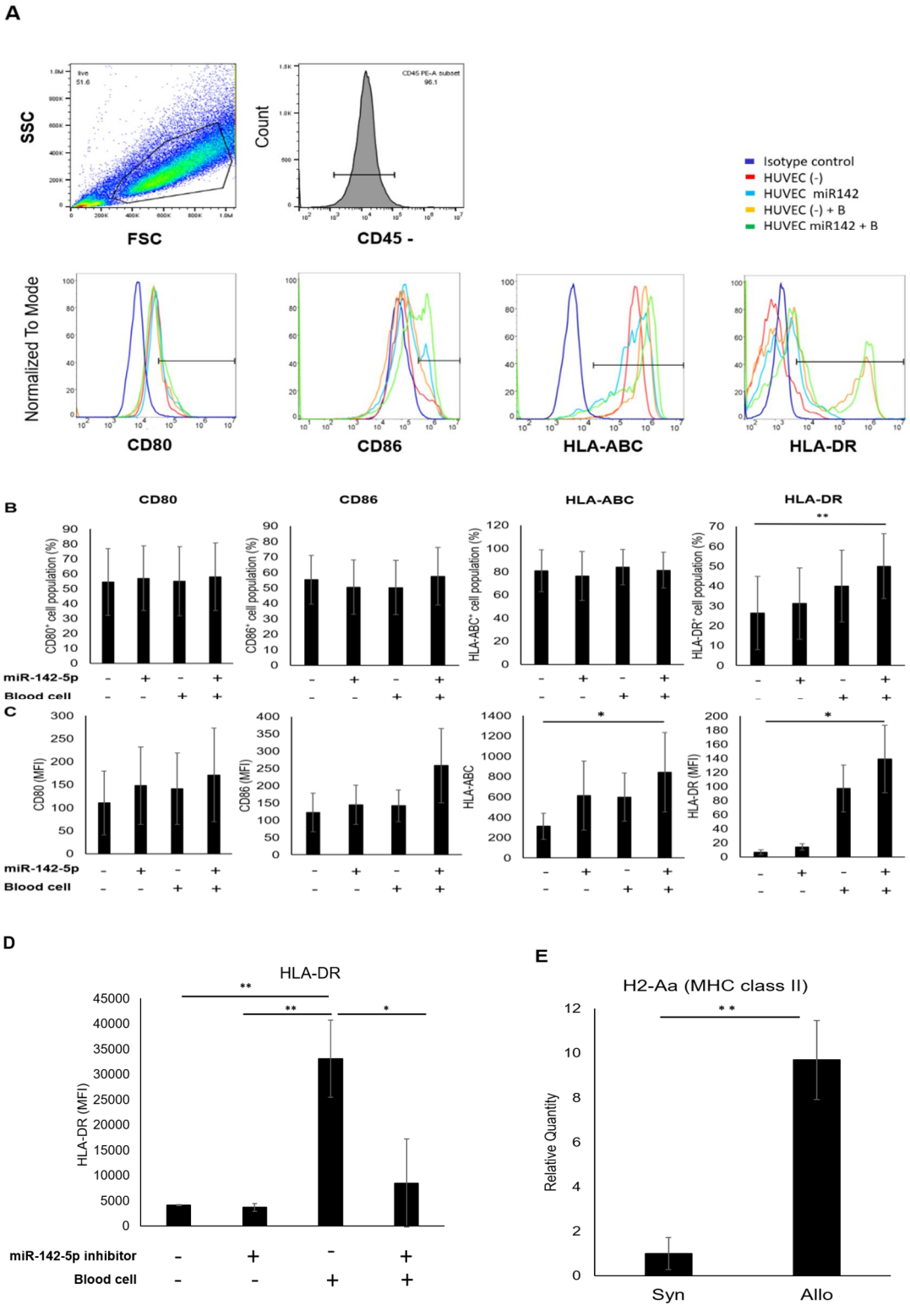
A
SSC
FSC
Count
CD45 -
Isotype control
HUVEC (-)
HUVEC miR142
HUVEC (-) + B
HUVEC miR142 + B
Normalized To Mode
CD80
CD86
HLA-ABC
HLA-DR
B
CD80
CD86
HLA-ABC
HLA-DR
CD80+ cell population (%)
CD86+ cell population (%)
HLA-ABC+ cell population (%)
HLA-DR+ cell population (%)
miR-142-5p
Blood cell
C
CD80 (MFI)
CD86 (MFI)
HLA-ABC
HLA-DR (MFI)
D
HLA-DR
HLA-DR (MFI)
miR-142-5p inhibitor
Blood cell
E
H2-Aa (MHC class II)
Relative Quantity
Syn
Allo

Figure 2. MHC class I and II are upregulated in HUVEC by miR-142-5p overexpression upon allogeneic immune responses. (A) The surface expression of T cell co-stimulatory molecules (CD80 and CD86) and MHC class I and II (HLA-ABC and HLA-DR) was measured on HUVEC by flow cytometry. HUVEC (-), mock-infected HUVEC line; HUVEC miR-142, miR-142-5p-expressing lentivirus-infected HUVEC cell line; **B**, blood mononuclear cells. Representative histograms are displayed out of 4 independent experiments. **(B)** The graphs show the percentages (mean ± SEM) of each surface molecule-positive cell population. N = 4. **(C)** The graphs show the mean fluorescence indices (mean ± SEM) of expression of each surface molecule. N = 4. **(D)** The surface expression of MHC class II (HLA-DR) was measured on HUVEC following the treatment of miR-142-5p inhibitor. N = 3. **(E)** The results of real-time qPCR demonstrated the upregulation of H2-Aa (MHC class II) gene expression in the allogeneic skin graft in mice. N = 3. *$P < 0.05$; **$P < 0.01$.

Figure 3.

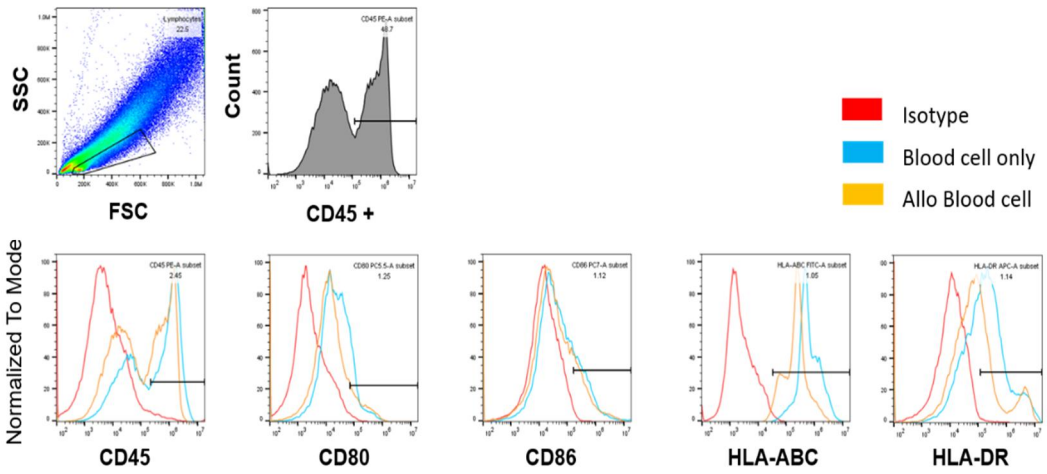

Figure 3. The expression of MHC molecules is not changed in blood cells by allogeneic immune responses.

The surface expression of T cell co-stimulatory molecules (CD80 and CD86) and MHC class I and II (HLA-ABC and HLA-DR) was measured on blood cells by flow cytometry.

ZEB1 is a target gene of miR-142-5p

Finally, I aimed to identify the target gene(s) regulated by miR-142-5p. The putative mRNA targets for miR-142-5p were identified using an on-line prediction database, miRTarBase (National Chiao Tung University Hsinchu, Taiwan). In Fig. 4A, the secondary structure of pre-miR-142-5p and cognate binding sites are displayed. Among the suggested putative target genes, the 3′ UTR of *ZEB1* had three miRanda-predicted binding sites for miR-142-5p (Fig. 4B). Hence, further investigations were focused on ZEB1. The expression of ZEB1 transcripts was downregulated in HUVEC in response to allogeneic condition. As miR-142-5p showed a higher upregulation on culture day 1 compared to day 3, an expected decrease in ZEB1 mRNA levels was observed on culture day 1 (Fig. 4C). Allogeneic skin graft also expressed less ZEB1 transcripts as well as protein, compared with those of syngeneic grafts (Fig. 4D and E). To further confirm the inhibitory effect of miR-142-5p on ZEB1 expression, HUVEC line was infected with miR-142-5p-expressing lentivirus, which excludes other possible pathways to regulate ZEB1 expression. The expression of miR-142-5p increased as expected (Fig. 5A) and ZEB1 expression decreased in HUVEC infected with miR-142-5p-

expressing lentivirus (Fig. 5B). On the contrary, The ZEB1 expression was increased when HUVEC were transfected with miR-142-5p inhibitor (Fig. 5C, D). In conclusion, miR-142-5p was upregulated, which consequently downregulated ZEB1 expression, in the early stage of rejection.

Figure 4.

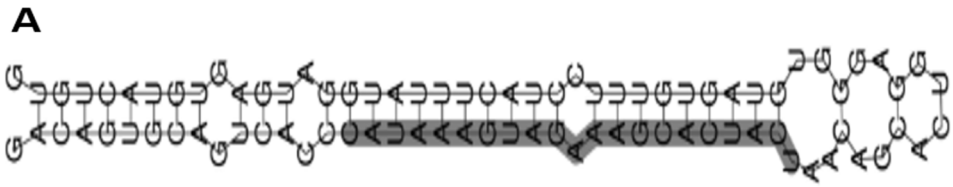

B

1	miR-142-5p ZEB1 (1107-1128 bp)	3'ucaucACGA AAGAUGAAAUAc 5' 5'aaattTTCTAATCTGCTTTATc 3'
2	miR-142-5p ZEB1 (1047-1067 bp)	3'ucaucaCGAAAGAUGAAAUAc 5' 5'ttcctcGGTATTGATTTTATg 3'
3	miR-142-5p ZEB1 (544-566 bp)	3'ucauCACGAAAGAUG--AAAUAc 5' 5'acccGTGCTAACTACCTTTTATa 3'

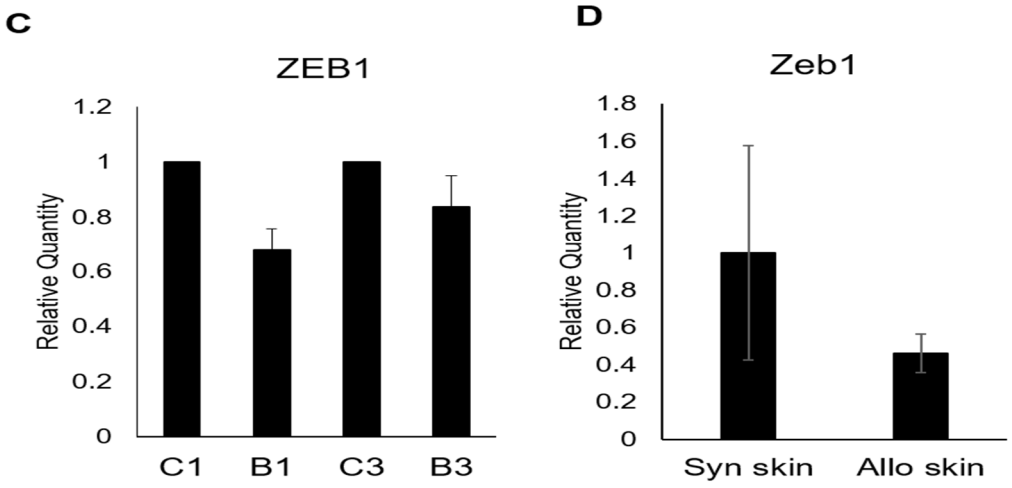

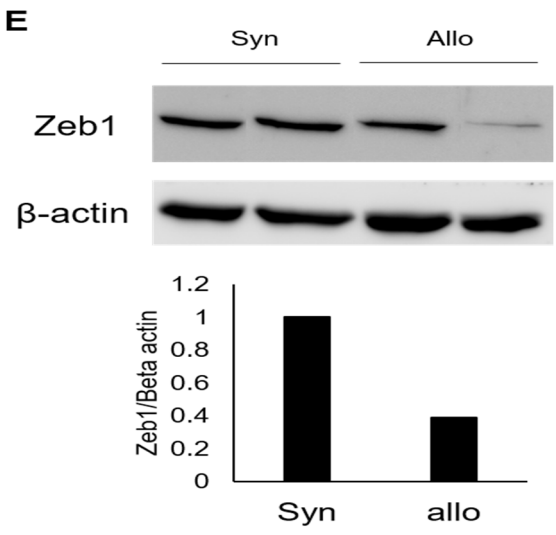

Figure 4. ZEB1 is a target gene of miR-142-5p. (A) The secondary structure of pre miR-142-5p is displayed by miRTarBase. The seed region of miR-142-5p is marked in red. (B) Three predicted *ZEB1* 3′ UTR putative binding sites of miR-142-5p. (C) The relative amount of ZEB1 mRNA was reduced in immortalized HUVEC upon co-culture with allogeneic blood cells. C, negative control; B, allogeneic blood mononuclear cells. The numeric values represent culture days. N = 3. (D) The relative amount of Zeb1 mRNA was reduced in allogeneic skin graft in mice. N = 4. (E) The amount of Zeb1 protein was reduced in allogeneic skin graft in mice. N = 2.

Figure 5.

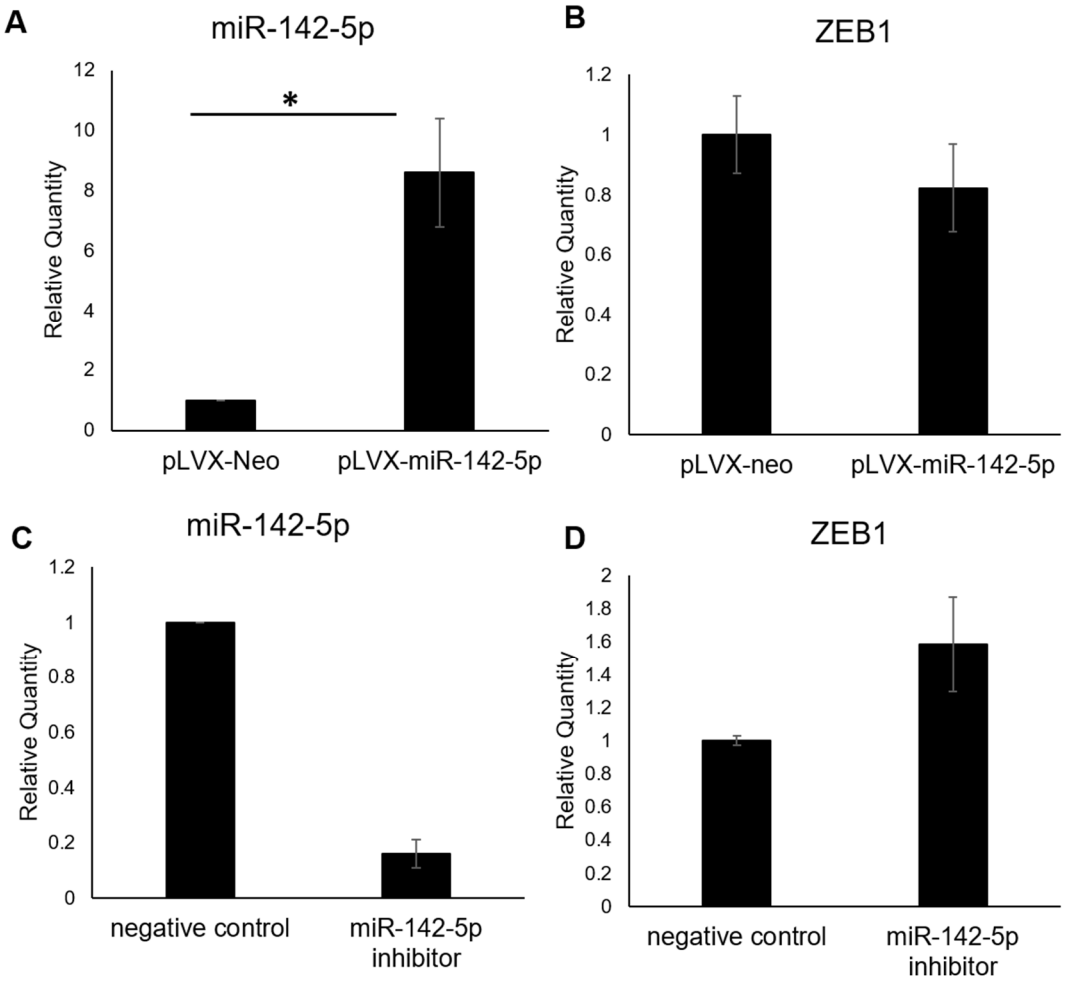
A
miR-142-5p
Relative Quantity
12
10
8
6
4
2
0
*
pLVX-Neo
pLVX-miR-142-5p
B
ZEB1
Relative Quantity
1.2
1
0.8
0.6
0.4
0.2
0
pLVX-neo
pLVX-miR-142-5p
C
miR-142-5p
Relative Quantity
1.2
1
0.8
0.6
0.4
0.2
0
negative control
miR-142-5p inhibitor
D
ZEB1
Relative Quantity
2
1.8
1.6
1.4
1.2
1
0.8
0.6
0.4
0.2
0
negative control
miR-142-5p inhibitor

Figure 5. **miR-142-5p overexpression reduces ZEB1 expression in HUVEC.** miR-142-5p-overexpressing HUVEC line was produced by lentiviral vector. (A) The overexpression of miR-142-5p was confirmed by TaqMan assay pLVX-Neo, mock-infected HUVEC line; miR-142-5p, miR-142-5p-overexpressing HUVEC line. N = 5. *P < 0.05. (B) ZEB1 expression was downregulated by miR-142-5p overexpression in HUVEC. Real time qPCR was performed to assess ZEB1 mRNA levels. N = 2. (C) miRNA downregulation was confirmed in miR-142-5p inhibitor-transfected HUVEC. (D) ZEB1 expression was upregulated in miR-142-5p inhibitor-transfected HUVEC.

Expression of miR-34c-5p is upregulated in hind limb ischemia and c-Myc is a target gene of miR-34c-5p.

miR-34c-5p was upregulated 12.4-fold in a biopsy sample collected from a CAV patient 1 month post operation, compared with that of a healthy heart transplant. Hypoxia was elicited by using hypoxic chamber and by treating H_2O_2. I confirmed the increase of miR-34c-5p in a hind limb ischemia model. The ligated tissues expressed significantly more miR-34c-5p, compared with those of sham (Fig. 6A). The hind limb tissues from the mice with hind limb ischemia showed marked damages in morphology at 1 day and 3 days after ligation, while the sham did not (Fig. 6B). The results were also confirmed in HUVEC upon hypoxia *in vitro* (Fig. 6C). The histology showed that hind limb ischemia was performed adequately. The secondary structure of pre-miR-34c-5p and cognate binding sites are displayed (Fig. 7A). Among the suggested putative target genes, the 3′ UTR of *c-MYC* had three miRanda-predicted binding sites for miR-34c-5p (Fig. 7B). To further confirm the inhibitory effect of miR-34c-5p, the HUVEC line was infected with miR-34c-5p-expressing

lentivirus. The expression of miR-34c-5p increased as expected (Fig. 7C). Accordingly, c-MYC protein level was decreased in miR-34c-5p overexpressing HUVEC (Fig. 7D).

Figure 6.

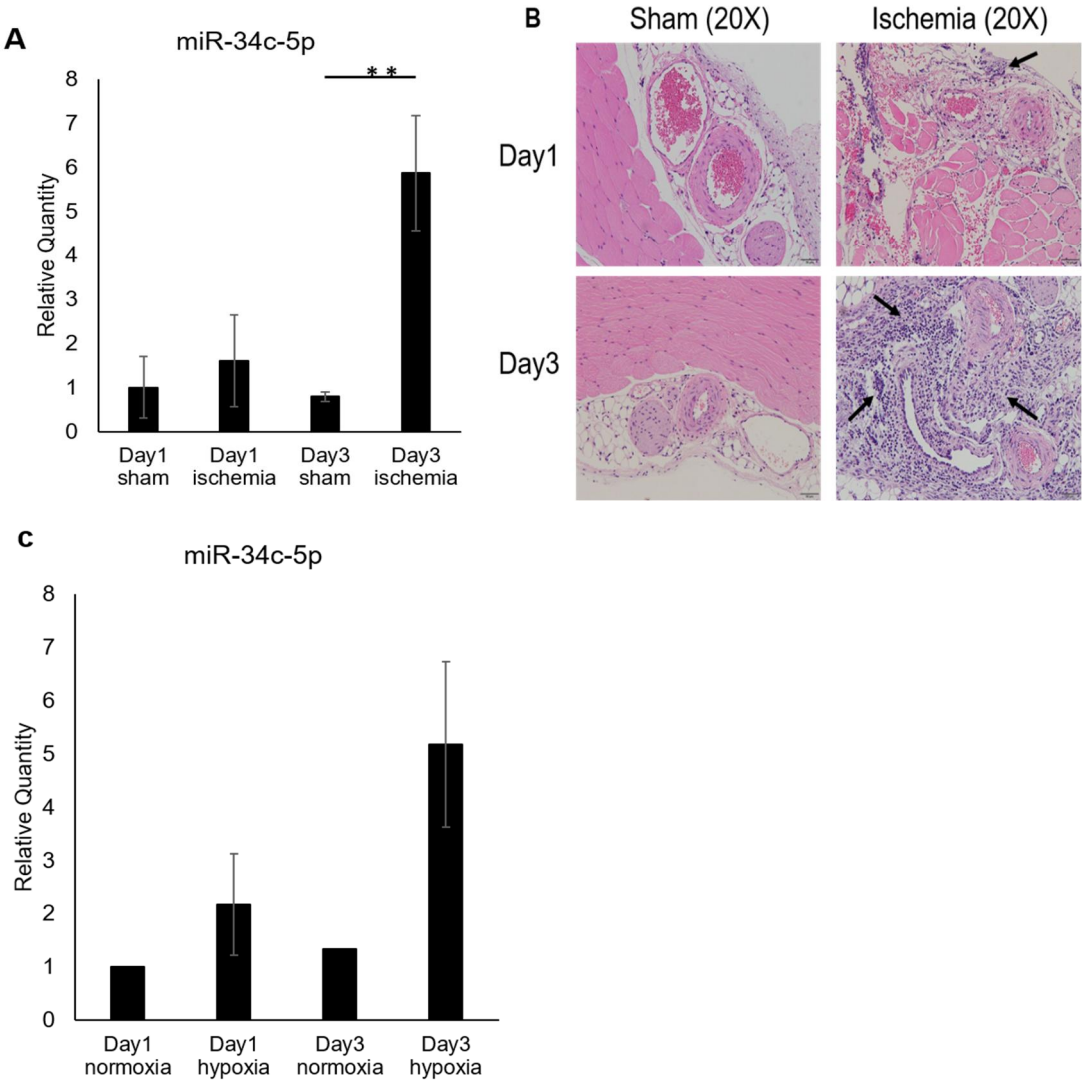
A
miR-34c-5p
* *
Relative Quantity
0
1
2
3
4
5
6
7
8
Day1 sham
Day1 ischemia
Day3 sham
Day3 ischemia
B
Sham (20X)
Ischemia (20X)
Day1
Day3
C
miR-34c-5p
Relative Quantity
0
1
2
3
4
5
6
7
8
Day1 normoxia
Day1 hypoxia
Day3 normoxia
Day3 hypoxia

Figure 6. **Expression of miR-34c-5p is upregulated in hypoxia *in vitro* and *in vivo*.** (A) TaqMan assay was performed to quantify miR-34c-5p in Hind limb ischemia model. The mice hind limb vessels were ligated for 1 and 3 days. The relative quantities of each miRNA are calculated as relative quantities of miRNAs to the sham control and displayed as ratios to the control (mean ± SD). N = 3 for each group. miR-34c-5p-overexpressing primary HUVEC was produced by lentiviral vector. (B) Representative histological results are shown as H & E-stained hind limb sections from sham and ischemic mice. Necrotic areas are defined by the presence of multi-cellular infiltrate (arrows). (C) TaqMan assay was performed to quantify miR-34c-5p in HUVECs cultured in a hypoxia chamber. HUVECs were harvested for 24h and 72h. N = 1 for negative HUVECs, N = 3 for 24h and 72h hypoxia HUVECs.

Figure 7.

B

1	miR-34c-5p c-MYC (119-144bp)	3’ cgUUAGUCG—AUUG-AUGUGACGGa 5’ 5’ agATTTAGCCATAATGTAAACTGCCt 3’
2	miR-34c-5p c-MYC (257-276bp)	3’ cguuAGUCGAUUGAUGUGACGGa 5’ 5’ tttcTCTG-TAA—ATATTGCCa 3’
3	miR-34c-5p c-MYC (442-466bp)	3’ cgUUAGUCGAUUG-AU-GUGACgga 5’ 5’ atAACTGGCAAATATATCATTGagc 3’

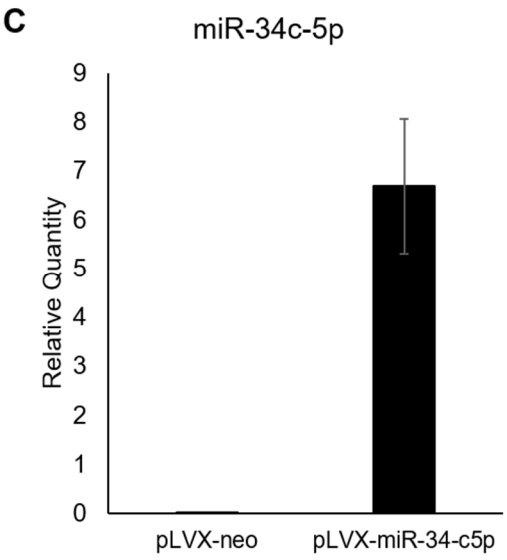

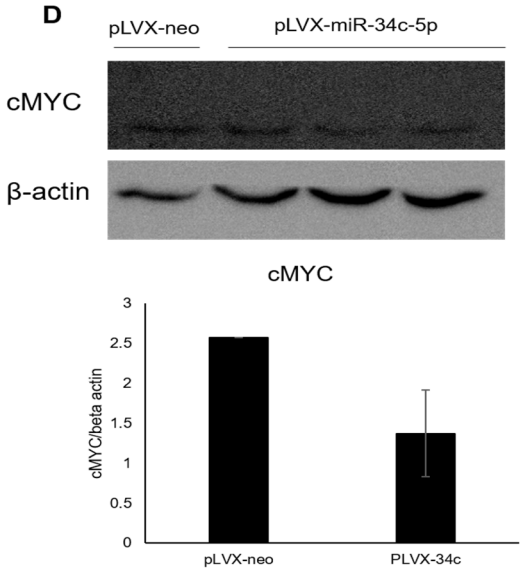

Figure 7.**c-MYC is a target gene of miR-34c-5p.**

(A) The secondary structure of pre miR-34c-5p is displayed by miRTarBase. The seed region of miR-34c-5p is marked in red. (B) Three predicted *c-MYC* 3′ UTR putative binding sites of miR-34c-5p. (C) The overexpression of miR-34c-5p was confirmed by TaqMan assay on pLVX-Neo, mock-infected HUVEC line; pLVX-miR-34c-5p, miR-34c-5p-overexpressing primary HUVEC. N = 2. (D) The amount of c-MYC protein was reduced in miR-34c-5p-overexpressing primary HUVEC. N = 1 for pLVX-neo, N = 3 for pLVX-miR-34c-5p.

Discussion

In this thesis, I demonstrate differential roles of miR-34c-5p and miR-142-5p in cardiac allograft vasculopathy using *in vitro* and *in vivo* experimental models. miR-142-5p was upregulated in HUVEC and skin graft upon allogeneic immune responses, while miR-34c-5p was upregulated in HUVEC in hypoxic environment and hind limb ischemia.

The overexpression of miR-142-5p, upregulated the expression of MHC class I and II in HUVEC. An increased expression of MHC class I and II in HUVEC and skin graft could

f

a

c

i

l

i

t ZEB1 is an E-cadherin repressor that promotes metastasis by inducing epithelial-

mesenchymal transition (EMT) [38]. miR-200 family, miR-205, and miR-150 are known to

t

e

regulate ZEB1 [39-41]. In particular, miR-200c and miR-150 have been shown to play an important role in the differentiation of human embryonic stem cells to endothelial cells by targeting ZEB1 [40]. ZEB1 represses the endothelial cell gene expression through direct binding to the promoters, consequently inhibiting vasculogenesis [40]. Endothelial-mesenchymal transition contributes to the development of various cardiovascular diseases, such as myocardial infarction, cardiac fibrosis, valve calcification, endocardial elastofibrosis, atherosclerosis, and pulmonary arterial hypertension [42], suggesting a potential role of ZEB1 in CAV. ZEB1 by itself downregulates miR-34a expression, driving prometastatic actin cytoskeletal remodeling [43]. In our microarray results (data not shown), the expression of miR-200b-3p and miR-200c-5p increased 3.5 and 2.6 fold, respectively, that was considerably less compared to that of miR-142-5p (11.7 fold), hence the effect of other miRNAs on ZEB1 gene could be lesser than that of miR-142-5p. ZEB1 containing a p300/CBP-associated factor (P/CAF) binding domain [38], and CIITA, a crucial transcription factor for MHC class II expression, recruits p300/CBP complex [44]. Thus, it is plausible that reduction of ZEB1, a transcription repressor, might promote MHC II transcription. Although, there are hitherto no

published results which directly proves the role of ZEB1 in MHC I or II gene expression, a recent report suggests that reduced expression of HLA-G homolog Qa-2 is associated with EMT where ZEB1 is upregulated [45].

The endomyocardial biopsies from patients with acute cellular rejection post cardiac transplantation show 4.8 fold increased miR-142-5p [21]. The biopsy samples are collected at least 6 weeks after transplantation. In mice, miR-142-5p is 2.28 or 13.54 fold increased in allogeneic heart grafts 7 days after transplantation [20, 21]. It is intriguing that miR-142-5p is upregulated in T cells activated by anti-CD3/CD28 mAbs, but rather downregulated in allogeneic T cells [46] and that miR-142-5p is not listed as upregulated in graft-infiltrated lymphocytes [20]. In line with those reports, miR-142-5p is more expressed in naïve T cells than effector and memory T cells when splenocytes from a TCR-transgenic mouse are *in vitro* activated with specific peptides [47], suggesting that miR-142-5p expression is not upregulated in antigen-specifically activated T cells. In addition, miR-142-5p was not upregulated in HUVEC cultured in hypoxia or with cyclosporine A (data not shown). Taken together, the increased miR-142-5p in the biopsy sample from a CAV patient was not likely

result of infiltrated immune cells, but was most likely due to endothelial activation upon allogeneic immune response.

During organ donation, organs are exposed hypoxia. Hypoxia-inducible factors (HIF) are the oxygen sensitive transcription factors that regulate many hypoxia-related genes [48]. Hypoxic stress induces signaling proteins and transcription factors change in order to regulate cellular functions and some studies prove that miRNAs are currently a key component in the response to hypoxia [49]. miR-21 has a protective role in cardiac ischemia/reperfusion injury. When *in vitro* and *in vivo* hypoxic stress occurs, miR-21 is upregulated and inhibits cardiac cell apoptosis induced by hypoxia (ischemia) / reperfusion injury, targeting PDCD4, which is a critical mediator for cancer cell apoptosis [50]. miR-26a is upregulated in H_2O_2-treated cardiomyocytes, and cell apoptosis and the expression of pro-apoptotic signal molecules are increased by downregulation of GSK-3β which is the target gene of miR-26a [51]. Conversely, some miRNAs are downregulated by hypoxia. In renal fibrosis, hypoxia-induced renal tubular cell EMT is a crucial incident [52]. Expression of miR-34a in renal tubular epithelial cells is downregulated by hypoxia and Notch1 and Jagged1 are target genes of miR-34a, that promote

EMT and renal fibrosis [52]. Xiaojian, et al. find miR-34c-5p is upregulated in the lung and the pulmonary smooth muscle cells by hypoxia and targets soluble guanylyl cyclase β1 (sGC β1). In their study, miR-34c-5p is not affected by HIF-1-α, but Sp1 [53].

c-Myc, referred to as MYC, is a regulator gene and proto-oncogen that codes for transcription factors. c-Myc regulates cell proliferation, senescence, angiogenesis and metabolism [54]. In normal proliferation cells, c-Myc mRNA and protein expression levels are low [55], but it is overexpressed in cancer cells [56]. Many studies prove that the relation between c-Myc and hypoxia [57-62]. Cardiac progenitor cells (CPCs), which promote cardiac regeneration and improve heart function, are impaired in hypoxia [59]. Hypoxic stress does not induce CPC death or senescence nor affect CPC differentiation, but impairs vasculogenesis and induces CPC quiescence [59]. Following CPC functional decline, c-Myc expression is reduced and affected protein stability [59]. In cancer studies, Nickel (Ni) compound and hypoxia cause cancer in humans and animal models [57]. Ni compounds mimic hypoxia and stabilize HIF-1-α and HIF-2- α , and c-Myc is degraded, resulting in decreased USP28 which is c-Myc de-ubiquinating enzyme [57]. In Human pulmonary endothelial cells, TFAM, a key

mitochondrial transcription factor, is decreased by hypoxia and HIF-2-α suppresses TFAM by decreasing c-Myc expression [62]. In addition, HIF-2-α, but not HIF-1-α, is accumulated in colon cancer cells by chronic hypoxia, and c-Myc and its downstream molecule cyclinD1 levels were increased in chronic hypoxia following knockdown of *HIF2A* [61].

In conclusion, miR-142-5p and miR-34c-5p are involved in rejection and hypoxic damage, respectively. It should be noted that the transcriptiomics was performed with biopsy samples only 1 month after transplantation. Thus, these miRNAs could be potential early diagnostic biomarkers for CAV.

References

[1] Taylor DO, Edwards LB, Boucek MM, Trulock EP, Waltz DA, Keck BM, et al. Registry of the International Society for Heart and Lung Transplantation: twenty-third official adult heart transplantation report--2006. The Journal of heart and lung transplantation : the official publication of the International Society for Heart Transplantation. 2006;25:869-79.

[2] Lund LH, Edwards LB, Kucheryavaya AY, Dipchand AI, Benden C, Christie JD, et al. The Registry of the International Society for Heart and Lung Transplantation: Thirtieth Official Adult Heart Transplant Report--2013; focus theme: age. The Journal of heart and lung transplantation : the official publication of the International Society for Heart Transplantation. 2013;32:951-64.

[3] Colvin-Adams M, Agnihotri A. Cardiac allograft vasculopathy: current knowledge and future direction. Clin Transplant. 2011;25:175-84.

[4] Chih S, Chong AY, Mielniczuk LM, Bhatt DL, Beanlands RSB. Allograft Vasculopathy. The Achilles' Heel of Heart Transplantation. 2016;68:80-91.

[5] Merola J, Jane-Wit DD, Pober JS. Recent advances in allograft vasculopathy. Curr Opin

Organ Transplant. 2017;22:1-7.

[6] Lim JY, Jung SH, Kim MS, Park JJ, Yun TJ, Kim JJ, et al. Cardiac allograft vasculopathy after heart transplantation: Is it really ominous? Clin Transplant. 2017;31.

[7] Gramley F, Lorenzen J, Pezzella F, Kettering K, Himmrich E, Plumhans C, et al. Hypoxia and myocardial remodeling in human cardiac allografts: a time-course study. The Journal of heart and lung transplantation : the official publication of the International Society for Heart Transplantation. 2009;28:1119-26.

[8] Yamani MH, Haji SA, Starling RC, Tuzcu EM, Ratliff NB, Cook DJ, et al. Myocardial ischemic-fibrotic injury after human heart transplantation is associated with increased progression of vasculopathy, decreased cellular rejection and poor long-term outcome. Journal of the American College of Cardiology. 2002;39:970-7.

[9] Buja LM. Myocardial ischemia and reperfusion injury. Cardiovascular pathology : the official journal of the Society for Cardiovascular Pathology. 2005;14:170-5.

[10] Du JK, Cong BH, Yu Q, Wang H, Wang L, Wang CN, et al. Upregulation of microRNA-22 contributes to myocardial ischemia-reperfusion injury by interfering with the mitochondrial

function. Free radical biology & medicine. 2016;96:406-17.

[11] Semenza GL. Hypoxia-inducible factor 1 and cardiovascular disease. Annual review of physiology. 2014;76:39-56.

[12] Harris A, Krams SM, Martinez OM. MicroRNAs as immune regulators: implications for transplantation. American journal of transplantation : official journal of the American Society of Transplantation and the American Society of Transplant Surgeons. 2010;10:713-9.

[13] Mas VR, Dumur CI, Scian MJ, Gehrau RC, Maluf DG. MicroRNAs as biomarkers in solid organ transplantation. American journal of transplantation : official journal of the American Society of Transplantation and the American Society of Transplant Surgeons. 2013;13:11-9.

[14] O'Connell RM, Rao DS, Baltimore D. microRNA regulation of inflammatory responses. Annual review of immunology. 2012;30:295-312.

[15] Bartel DP. MicroRNAs: genomics, biogenesis, mechanism, and function. Cell. 2004;116:281-97.

[16] Ambros V. The functions of animal microRNAs. Nature. 2004;431:350-5.

[17] Yates LA, Norbury CJ, Gilbert RJ. The long and short of microRNA. Cell. 2013;153:516-9.

[18] Guo H, Ingolia NT, Weissman JS, Bartel DP. Mammalian microRNAs predominantly act to decrease target mRNA levels. Nature. 2010;466:835-40.

[19] Sui W, Dai Y, Huang Y, Lan H, Yan Q, Huang H. Microarray analysis of MicroRNA expression in acute rejection after renal transplantation. Transpl Immunol. 2008;19:81-5.

[20] Wei L, Wang M, Qu X, Mah A, Xiong X, Harris AG, et al. Differential expression of microRNAs during allograft rejection. American journal of transplantation : official journal of the American Society of Transplantation and the American Society of Transplant Surgeons. 2012;12:1113-23.

[21] Van Aelst LN, Summer G, Li S, Gupta SK, Heggermont W, De Vusser K, et al. RNA Profiling in Human and Murine Transplanted Hearts: Identification and Validation of Therapeutic Targets for Acute Cardiac and Renal Allograft Rejection. American journal of transplantation : official journal of the American Society of Transplantation and the American Society of Transplant Surgeons. 2016;16:99-110.

[22] Gupta SK, Itagaki R, Zheng X, Batkai S, Thum S, Ahmad F, et al. miR-21 promotes fibrosis in an acute cardiac allograft transplantation model. Cardiovasc Res. 2016;110:215-26.

[23] el Azzouzi H, Leptidis S, Dirkx E, Hoeks J, van Bree B, Brand K, et al. The hypoxia-inducible microRNA cluster miR-199a approximately 214 targets myocardial PPARdelta and impairs mitochondrial fatty acid oxidation. Cell metabolism. 2013;18:341-54.

[24] Zhang A, Wang K, Zhou C, Gan Z, Ma D, Ye P, et al. Knockout of microRNA-155 ameliorates the Th1/Th17 immune response and tissue injury in chronic rejection. The Journal of heart and lung transplantation : the official publication of the International Society for Heart Transplantation. 2017;36:175-84.

[25] Singh N, Heggermont W, Fieuws S, Vanhaecke J, Van Cleemput J, De Geest B. Endothelium-enriched microRNAs as diagnostic biomarkers for cardiac allograft vasculopathy. The Journal of heart and lung transplantation : the official publication of the International Society for Heart Transplantation. 2015;34:1376-84.

[26] Neumann A, Napp LC, Kleeberger JA, Benecke N, Pfanne A, Haverich A, et al. MicroRNA 628-5p as a Novel Biomarker for Cardiac Allograft Vasculopathy. Transplantation.

2017;101:e26-e33.

[27] Ha CH, Lee SC, Kim S, Chung J, Bae H, Kwon K. Novel mechanism of gene transfection by low-energy shock wave. Scientific reports. 2015;5:12843.

[28] Rovira J, Sabet-Baktach M, Eggenhofer E, Lantow M, Koehl GE, Schlitt HJ, et al. A color-coded reporter model to study the effect of immunosuppressants on CD8+ T-cell memory in antitumor and alloimmune responses. Transplantation. 2013;95:54-62.

[29] Drake JM, Strohbehn G, Bair TB, Moreland JG, Henry MD. ZEB1 enhances transendothelial migration and represses the epithelial phenotype of prostate cancer cells. Molecular biology of the cell. 2009;20:2207-17.

[30] Ju MJ, Qiu SJ, Fan J, Xiao YS, Gao Q, Zhou J, et al. Peritumoral activated hepatic stellate cells predict poor clinical outcome in hepatocellular carcinoma after curative resection. American journal of clinical pathology. 2009;131:498-510.

[31] Kim YJ, Kim NY, Lee MK, Choi HJ, Baek HJ, Nam CH. Overexpression and unique rearrangement of VH2 transcripts in immunoglobulin variable heavy chain genes in ankylosing spondylitis patients. Experimental & molecular medicine. 2010;42:319-26.

[32] Siles L, Sanchez-Tillo E, Lim JW, Darling DS, Kroll KL, Postigo A. ZEB1 imposes a temporary stage-dependent inhibition of muscle gene expression and differentiation via CtBP-mediated transcriptional repression. Molecular and cellular biology. 2013;33:1368-82.

[33] Biswas A, Meissner TB, Kawai T, Kobayashi KS. Cutting edge: impaired MHC class I expression in mice deficient for Nlrc5/class I transactivator. Journal of immunology (Baltimore, Md : 1950). 2012;189:516-20.

[34] Yuan J, Crittenden RB, Bender TP. c-Myb promotes the survival of CD4+CD8+ double-positive thymocytes through upregulation of Bcl-xL. Journal of immunology (Baltimore, Md : 1950). 2010;184:2793-804.

[35] Shi-Bai Z, Rui-Min L, Ying-Chuan S, Jie Z, Chao J, Can-Hua Y, et al. TIPE2 expression is increased in peripheral blood mononuclear cells from patients with rheumatoid arthritis. Oncotarget. 2017;8:87472-9.

[36] Arora S, Gullestad L. The challenge of allograft vasculopathy in cardiac transplantation. Curr Opin Organ Transplant. 2014;19:508-14.

[37] Weis M, von Scheidt W. Cardiac allograft vasculopathy: a review. Circulation.

1997;96:2069-77.

[38] Zhang P, Sun Y, Ma L. ZEB1: At the crossroads of epithelial-mesenchymal transition, metastasis and therapy resistance. Cell Cycle. 2015;14:481-7.

[39] Park SM, Gaur AB, Lengyel E, Peter ME. The miR-200 family determines the epithelial phenotype of cancer cells by targeting the E-cadherin repressors ZEB1 and ZEB2. Genes & Development. 2008;22:894-907.

[40] Luo Z, Wen G, Wang G, Pu X, Ye S, Xu Q, et al. MicroRNA-200C and -150 play an important role in endothelial cell differentiation and vasculogenesis by targeting transcription repressor ZEB1. Stem cells (Dayton, Ohio). 2013;31:1749-62.

[41] Gregory PA, Bert AG, Paterson EL, Barry SC, Tsykin A, Farshid G, et al. The miR-200 family and miR-205 regulate epithelial to mesenchymal transition by targeting ZEB1 and SIP1. Nature cell biology. 2008;10:593-601.

[42] Li Y, Lui KO, Zhou B. Reassessing endothelial-to-mesenchymal transition in cardiovascular diseases. Nat Rev Cardiol. 2018;15:445-56.

[43] Ahn YH, Gibbons DL, Chakravarti D, Creighton CJ, Rizvi ZH, Adams HP, et al. ZEB1

drives prometastatic actin cytoskeletal remodeling by downregulating miR-34a expression. J Clin Invest. 2012;122:3170-83.

[44] Choi NM, Majumder P, Boss JM. Regulation of major histocompatibility complex class II genes. Curr Opin Immunol. 2011;23:81-7.

[45] da Silva IL, Montero-Montero L, Martin-Villar E, Martin-Perez J, Sainz B, Renart J, et al. Reduced expression of the murine HLA-G homolog Qa-2 is associated with malignancy, epithelial-mesenchymal transition and stemness in breast cancer cells. Scientific reports. 2017;7:6276.

[46] Sun Y, Tawara I, Zhao M, Qin ZS, Toubai T, Mathewson N, et al. Allogeneic T cell responses are regulated by a specific miRNA-mRNA network. J Clin Invest. 2013;123:4739-54.

[47] Wu H, Neilson JR, Kumar P, Manocha M, Shankar P, Sharp PA, et al. miRNA profiling of naive, effector and memory CD8 T cells. PloS one. 2007;2:e1020.

[48] Akhtar MZ, Sutherland AI, Huang H, Ploeg RJ, Pugh CW. The role of hypoxia-inducible factors in organ donation and transplantation: the current perspective and future opportunities.

American journal of transplantation : official journal of the American Society of Transplantation and the American Society of Transplant Surgeons. 2014;14:1481-7.

[49] Nallamshetty S, Chan SY, Loscalzo J. Hypoxia: a master regulator of microRNA biogenesis and activity. Free radical biology & medicine. 2013;64:20-30.

[50] Cheng Y, Zhu P, Yang J, Liu X, Dong S, Wang X, et al. Ischaemic preconditioning-regulated miR-21 protects heart against ischaemia/reperfusion injury via anti-apoptosis through its target PDCD4. Cardiovascular research. 2010;87:431-9.

[51] Suh JH, Choi E, Cha M-J, Song B-W, Ham O, Lee S-Y, et al. Up-regulation of miR-26a promotes apoptosis of hypoxic rat neonatal cardiomyocytes by repressing GSK-3β protein expression. Biochemical and Biophysical Research Communications. 2012;423:404-10.

[52] Du R, Sun W, Xia L, Zhao A, Yu Y, Zhao L, et al. Hypoxia-induced down-regulation of microRNA-34a promotes EMT by targeting the Notch signaling pathway in tubular epithelial cells. PloS one. 2012;7:e30771.

[53] Xu X, Wang S, Liu J, Dou D, Liu L, Chen Z, et al. Hypoxia induces downregulation of soluble guanylyl cyclase β1 by miR-34c-5p. Journal of cell science. 2012;125:6117-26.

[54] Lüscher B, Larsson LG. The world according to MYC. Conference on MYC and the transcriptional control of proliferation and oncogenesis. EMBO reports. 2007;8:1110-4.

[55] Rudolph C, Adam G, Simm A. Determination of copy number of c-Myc protein per cell by quantitative Western blotting. Analytical biochemistry. 1999;269:66-71.

[56] Hann SR, Eisenman RN. Proteins encoded by the human c-myc oncogene: differential expression in neoplastic cells. Molecular and cellular biology. 1984;4:2486-97.

[57] Li Q, Kluz T, Sun H, Costa M. Mechanisms of c-myc degradation by nickel compounds and hypoxia. PloS one. 2009;4:e8531.

[58] Yu Y, Niapour M, Zhang Y, Berger SA. Mitochondrial regulation by c-Myc and hypoxia-inducible factor-1α controls sensitivity to econazole. Molecular Cancer Therapeutics. 2008;7:483.

[59] Bellio MA, Pinto MT, Florea V, Barrios PA, Taylor CN, Brown AB, et al. Hypoxic Stress Decreases c-Myc Protein Stability in Cardiac Progenitor Cells Inducing Quiescence and Compromising Their Proliferative and Vasculogenic Potential. Scientific reports. 2017;7:9702.

[60] Yoo YG, Hayashi M, Christensen J, Huang LE. An essential role of the HIF-1alpha-c-

Myc axis in malignant progression. Annals of the New York Academy of Sciences. 2009;1177:198-204.

[61] Wang L, Xue M, Chung DC. c-Myc is regulated by HIF-2α in chronic hypoxia and influences sensitivity to 5-FU in colon cancer. Oncotarget. 2016;7:78910-7.

[62] Zarrabi AJ, Kao D, Nguyen DT, Loscalzo J, Handy DE. Hypoxia-induced suppression of c-Myc by HIF-2α in human pulmonary endothelial cells attenuates TFAM expression. Cellular signalling. 2017;38:230-7.

국문요약

배경: 심장 동종 이식 혈관병증은 심장 이식 후 환자의 장기적인 생존을 제한하는 질환이다. Microarray 분석을 통해 건강한 심장이식 예후를 보이는 환자의 심장 조직과 비교하여 심장 동종 이식 혈관병증 환자의 심장조직에서 증가된 miRNA를 선택했다. 이전의 연구에서 miR-142-5p는 인간 탯줄 내피세포와 관련이 없는 혈액세포를 같이 배양하여 면역 반응이 일어났을 때 증가함을 보였고, 반면에 miR-34c-5p는 산소가 부족한 상태에서 증가함을 보였다. 따라서 이 연구는 생체 외, 생체 내에서 면역 반응과 저산소증에 관여하는 miRNA의 역할을 알아보기 위해 실험을 진행하였다.

방법: 면역 반응을 일으키기 위해 탯줄 내피세포와 혈액 세포를 같이 배양하였다. 탯줄 내피세포에 렌티바이러스 감염을 통해 miRNA를 과발현하게 만들었고 miRNA 억제제로 miRNA를 억제하는 실험을 진행하였다. 피부이식모델은 생쥐에 피부이식 해준 후 7 일 후에 희생시켰고 허벅지 혈관 허혈 모델은 혈관을 묶어준 후 1 일, 3 일 후에 생쥐를 희생시켰다. miRNA 및 mRNA의 발현은 qPCR을 통해 평가였다. 인간 탯줄 내피세포 표면의 B7-1 (CD80), B7-2 (CD86), MHC class I (HLA-

ABC) 및 II (HLA-DR)의 발현을 유세포 분석을 사용하여 분석하였다. 또한 이식한 피부와 허혈한 허벅지 혈관에서 단백질 발현은 western blotting으로 평가하였다.

결과: 인간 탯줄 내피세포와 혈액세포의 면역반응과 생쥐 피부이식 모델에서 이식거부반응에 의해 miR-142-5p가 상향 조절된다는 것을 확인하였다. MHC class I (HLA-ABC) 과 MHC class II (HLA-DR)을 발현하는 인간 탯줄 내피세포의 분포와 형광의 세기는 면역반응에 의해 증가하였고 생쥐 피부이식 모델의 이식편에서 MHC class II 유전자 (H2-Aa)의 발현이 증가함을 확인하였다. *ZEB1* 의 3' UTR에는 miR-142-5p에 대한 3 개의 결합 부위를 갖고 있음을 확인하였고 생체 외, 생체 내 실험에서 ZEB1 의 mRNA 수준과 단백질 수준은 면역반응에 의해 감소함을 확인하였다. miR-142-5p를 과발현하게 만든 인간 탯줄 내피세포에서 ZEB1 의 발현은 감소하였고 반면 인간 탯줄 내피세포에서 miR-142-5p를 억제하였을 시 ZEB1 의 발현이 증가함을 확인할 수 있었다. 또한, 생쥐 허벅지 혈관 허혈 모델과 인간 탯줄 내피세포에 dysoxia 유도는 miR-34c-5p의 발현을 증가시켰다. *c-Myc*의 3'UTR에는 miR-34c-5p에 대한 3 개의 결합 부위를 갖고 있음을

확인하였고 c-Myc의 단백질 수준은 miR-34c-5p를 과발현하게 만든 인간 탯줄 내피세포에서 감소함을 확인하였다.

결론: 생체 외, 생체 내 실험에서 면역반응에 의해 miR-142-5p가 증가하고 저산소증에 의해 miR-34c-5p가 증가함을 확인하였다. 면역 반응에 의해 증가된 miR-142-5p에 의해 ZEB1 은 감소하였고 miR-34c-5p에 의해 c-Myc은 감소하였다. 이러한 결과는 심장이식거부반응이 miR-142-5p와 miR-34c-5p의 발현 증가와 결과적으로 ZEB1 과 c-Myc의 발현 감소에 의해 악화될 수 있는 것으로 보인다.